Imaging of the protoelliptical NGC 1700 and its globular cluster system

Richard J. N. Brown, Duncan A. Forbes, Amarkus Kissler–Patig and Jean P. Brodie⁴

- 1 School of Physics and Astronomy, University of Birmingham, Edgbaston, Birmingham, B15 2TT, UK Email: rjnb, forbes@star.sr.bham.ac.uk
- ² Astrophysics & Supercomputing, Swinburne University of Technology, Hawthorn NSW 3122, Australia dforbes@swin.edu.au
- ³ ESO, Karl-Schwarzchild-Strasse 2, D-85748, Garching bei München, Germany mkissler@eso.org
- ⁴ Lick Observatory, University of California, Santa Cruz, CA 95064, USA brodie@ucolick.org

Accepted; Received; in original form

ABSTRACT

An excellent candidate for a young elliptical, or 'protoelliptical' galaxy is NGC 1700. Here we present new B, V and I band imaging using the Keck telescope and reanalyse existing V and I band images from the $Hubble\ Space\ Telescope$. After subtracting a model of the galaxy from the Keck images NGC 1700 reveals two symmetric tidal tail-like structures. If this interpretation is correct, it suggests a past merger event involving two spiral galaxies. These tails are largely responsible for the 'boxiness' of the galaxy isophotes observed at a radius of ~ 13 kpc.

We also show that the B-I colour distribution of the globular cluster system is bimodal. The mean colour of the blue population is consistent with those of old Galactic globular clusters. Relative to this old, metal poor population, we find that the red population is younger and more metal rich. This young population has a similar age and metallicity as that inferred for the central stars, suggesting that they are both associated with an episode of star formation triggered by the merger that may have formed the galaxy. Although possessing large errors, we find that the majority of the age estimates of NGC 1700 are reasonably consistent and we adopt a 'best estimate' for the age of 3.0 ± 1.0 Gyr. This relatively young age places NGC 1700 within the age range where there is a notable lack of obvious candidates for protoellipticals. The total globular cluster specific frequency is rather low for a typical elliptical, even after taking into account fading of the galaxy over the next 10 Gyr. We speculate that NGC 1700 will eventually form a relatively 'globular cluster poor' elliptical galaxy.

Key words: galaxies: elliptical – galaxies: individual – galaxies: evolution – galaxies: structure

1 INTRODUCTION

Merging is now thought to be a key process in the evolution of galaxies. The hypothesis that two colliding spiral galaxies will eventually form an elliptical galaxy (Toomre & Toomre 1972) has gained much observational and theoretical support over the years. The 'smoking gun' of this type of merger is the presence of two tidal tails, formed from the progenitor's discs. A number of well known examples are found in the local Universe, such as *The Mice*, *The Antennae*, Arp 220,

NGC 3256 and NGC 7252. For such galaxies a variety of methods are available (e.g. spectroscopy of the stellar populations, dynamical measurements, comparison with models etc.) to estimate the time since the merger occurred. The derived ages, for these classic tidal tail systems, is up to 1–2 Gyr since nuclear coalescence. It was Ivan King in 1977 who first pointed out the general lack of obvious candidates for older merger remnants (i.e. 2–5 Gyr old). These galaxies have been referred to as 'King gap objects' or protoellipticals. Identifying, and age dating, these protoellipticals could

provide the missing link between late stage spiral mergers and elliptical galaxies.

Indeed, a crucial step in testing the merger hypothesis would be to show an 'evolutionary consistency', i.e. that spiral mergers and protoellipticals evolve to have the same energetic, structural, dynamical and chemical properties as normal, old ellipticals. This has been problematic due to the difficulty of estimating the age of old stellar populations, without telltale morphological signatures such as tidal tails. Recently, several different methods have become available. These include breaking the age—metallicity degeneracy with spectral synthesis (e.g. Gonzalez 1992) and new models (e.g. Worthey 1994), quantifying optical fine structure (Schweizer & Seitzer 1992) and using the colours of globular clusters (e.g. Whitmore et al. 1997).

An ideal candidate for a nearby protoelliptical is NGC 1700. It possesses a kinematically distinct core (Franx, Illingworth & Heckman 1998a), reveals evidence for extensive morphological disturbance (Forbes & Thomson 1992) and it has a high rotational velocity to velocity dispersion ratio, relative to other ellipticals (Bender, Burstein & Faber 1992). As well as being a possible protoelliptical, it offers the opportunity to compare various age estimates. For example, age estimates can be made from its two faint tidal tails, optical fine structure, globular cluster colours, kinematic structure, and its stellar component.

We have adopted the same distance to NGC 1700 as Whitmore et al. (1997), i.e. 51.4 Mpc (which includes a correction for Virgocentric infall and assumes $H_{\circ}=75$ km s⁻¹ Mpc⁻¹). This corresponds to 249 pc per arcsec. The total B band magnitude for NGC 1700 is $M_{\rm B}=-21.56$ (RC3:de Vaucouleurs et al. 1991). It is classified as an E4 elliptical in the RC3 and E3 in the RSA. Photometric studies have been carried out by Franx, Illingworth & Heckman (1998b) and Goudfrooij et al. (1994). A recent kinematic study is that of Bender, Saglia & Gerhard (1994).

In this paper we reanalyse $Hubble\ Space\ Telescope\ (HST)\ WFPC2\ V,\ I$ images and present new Keck $B,\ V$ and I images. We focus on the morphology of the galaxy and photometry of the globular cluster system, both of which provide new age estimates. We compare our age estimates with a variety of alternative methods and discuss the implications of our results for the formation and evolution of elliptical galaxies.

2 OBSERVATIONS AND INITIAL DATA REDUCTION

2.1 Keck data

New B, V and I images of NGC 1700 were obtained using the 10 m Keck–I telescope at the W. M. Keck Observatory, Mauna Kea, Hawaii. The observations were carried out on 1997 September 30th, with seeing in each filter of ~ 1.3 arcsec. The LRIS instrument was used with the Tek 2048 \times 2048 CCD, giving a rectangular field–of–view of 6×8 arcmin and a pixel scale of 0.215 arcsec pixel⁻¹. A single long (600 s) exposure was taken in V and I filters and two 600 s exposures were taken in the B band. We also took a short (10 s) exposure in each filter. For the purpose of photometric calibration we obtained exposures in each filter of the field SA98 from Landolt (1992).

The data were reduced in a standard manner using IRAF software. After bias subtraction there remained a small offset between the two halves of the CCD. This is due to the dual amplifier mode of the CCD read-out. This effect is reasonably well approximated by a step function which varies perpendicular to the read-out direction. The bulk of this offset was successfully removed after division by the normalised flat-field. A small offset ($\sim 1-3$ per cent) remained, which was corrected for by multiplying one side by a factor determined by taking the mean values of several sky regions either side of the offset. This successfully removed the offset for most of the image. However, an offset remained in the bright regions at the very centre of the galaxy (\sim few arcsec). This may be due to some non-linearity in the gains of the amplifiers at high count rates (as suggested in the LRIS manual). This problem clearly affects galaxy photometry in the inner regions but as described below, does not affect standard star or globular cluster (GC) photometry.

Photometric calibration was performed using our standard star exposures of SA98 and the photometric measurements of Landolt (1992). The resulting rms error in the final photometry is ± 0.02 mag in all three bands. K-correction and Galactic extinction were included using the same values for NGC 1700 as in Goudfrooij et al. (1994), 0.18, 0.11 and 0.07 in the $B,\ V$ and I bands respectively. In order to investigate the random errors on our zeropoints we compared the measurements for the same stars that appear in each pointing. We found a random error of 0.02 mag. To better quantify the systematic error due to the dual amplifier offset, we compared the mean zeropoints for the stars on the left and stars on the right of the offset in the same frame. We found a systematic error due to the offset of 0.03 mag.

3 DATA ANALYSIS

3.1 HST data

The V and I band HST data of NGC 1700 were obtained from proposal G0–5416 in the HST archive. Photometry of the GCs in NGC 1700 has been discussed by Whitmore et al. (1997). Here we reanalyse the HST data, and use the results to aid with GC selection in our Keck data.

We performed the photometry in 2 pixel radius apertures with SEXTRACTOR (Bertin & Arnouts 1996), applying the aperture correction given by Whitmore et al. (1997) and the calibration and transformation to Johnson magnitudes following Holtzman et al. (1995).

From the initial object list of 383 sources detected by SEXTRACTOR we applied the following selection criteria: The magnitude range was restricted to be 21.5 < V < 26.5, the faint limit chosen to avoid introducing colour bias effects due to lack of completeness. Galactic GCs at the distance of NGC 1700 are expected to be at magnitudes of V > 22.5. However, in order to account for the possible presence of a younger population of GCs that might be up to ~ 1 mag brighter than those in the Milky Way, we relaxed our bright limit to be V = 21.5.

The object colours were restricted to 0.6 < V - I < 1.7 (which is roughly equivalent to -2.5 < [Fe/H] < +1). Our typical error is ± 0.1 in magnitude and ± 0.15 in colour. Finally we carried out a careful visual check of the objects

on the image display in order to remove point-like or galaxy-like objects. The final list contains a total of $146~\mathrm{GCs}$ from all $4~\mathrm{WFPC2}$ chips.

3.2 Keck data

3.2.1 Galaxy morphology

In order to better reveal the fine structure present within NGC 1700 it is necessary to subtract off a model of the underlying galaxy. All modelling was performed using the ISOPHOTE package in STSDAS (e.g. Forbes & Thomson 1992). We initially constructed a model for the purpose of sky subtraction. Elliptical isophotes were fitted with a fixed centre and employing a 3- σ clipping algorithm. The ellipticity and position angle of the isophotes were allowed to vary freely. A pixel mask file was also constructed to explicitly mask out stars and pixel defects. We were unable to perform fits for the long exposure images at small radii because the central regions were saturated. For these images we set the initial fit radius beyond the saturated region. The fits were allowed to progress outwards until constraints on signal to noise (S/N)terminated the process. Sky subtraction was performed in a similar way to that detailed in Goudfrooij et al. (1994), i.e. the model intensity profiles in the outer parts of the galaxy were fitted by a power-law in order to accurately determine the sky level. The appropriate level was then subtracted from each image. The sky-subtracted images were then re-modelled in an identical way to before, to reveal the structure within the body of the galaxy. The models typically reached out to a distance of ~ 180 arcsec (45 kpc) from the galaxy centre.

Our fits extend significantly further from the centre than the imaging of either Goudfrooij et al. (1994) or Franx et al. (1989b). Using the short exposure image, we estimate a total B band magnitude for the galaxy of 12.00 ± 0.05 , in excellent agreement with that given by the RC3 of 12.01. We also estimate a total V magnitude of 11.18 ± 0.05 which agrees reasonably well with the RC3 value of 11.10, and a total I magnitude of 9.80 ± 0.10 compared with 9.87 from Poulain (1988).

We show in Fig. 1 the radial profiles of the ellipticity, position angle (PA), third cosine term (C3) and the fourth cosine term (C4) of the fitted isophotes for the short B band image. All radii are expressed in terms of 'equivalent radius', $r_{\rm eq} = a\sqrt{1-\epsilon}$, where a is the major axis radius and ϵ is the isophote ellipticity. The C4 term is perhaps the most interesting of a Fourier series which expresses the deviations from a pure ellipse at a given radius. This term describes whether the isophotes are discy (C4 is positive) with excess light along the major and/or minor axes, or boxy (C4 is negative), representing excess light at 45° with respect to these axes. There is good agreement between the shape and absolute values of our data and that of Goudfrooij et al. (1994) and Franx et al. (1989b). The slight discrepancies at small radii are almost certainly due to seeing effects. Our profiles in V and I were similar in both shape and absolute value to that in the B band.

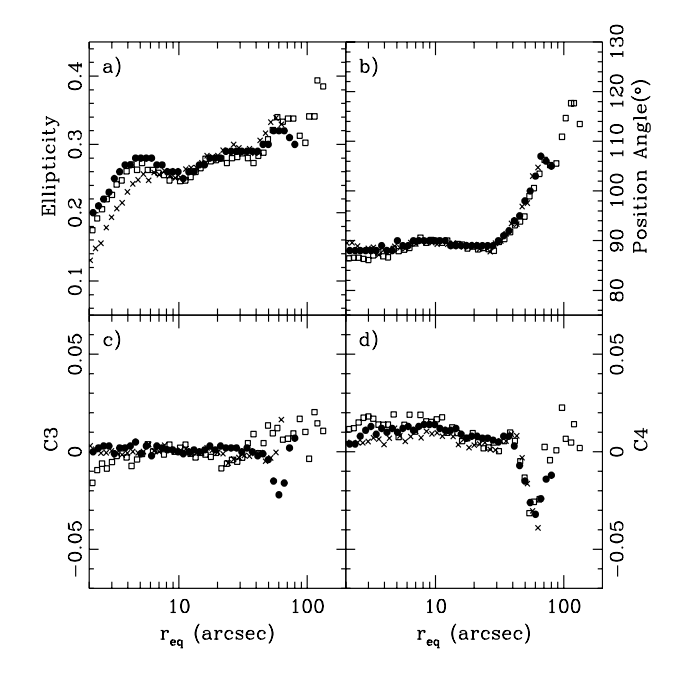


Figure 1. Radial profiles of the fit to our short B band exposure (open squares) in terms of equivalent radius $(r_{\rm eq}=a\sqrt{1-\epsilon})$. For comparison, the profiles of Goudfrooij et al. (1994) and Franx et al. (1989b) are shown as crosses and solid circles respectively. Our results agree well with these previous studies but extend to larger radii.

$\it 3.2.2 \quad Globular\ cluster\ sample\ selection\ and\ photometry$

As with the HST data, potential GC candidates were detected in the Keck images using the SEXTRACTOR program. SEXTRACTOR provides measures of FWHM, ellipticity and an indication of whether an object was 'pointy' (star-like) or extended (galaxy-like). We found 615 candidates in common between the B, V and I band images. Using this object list, we performed photometry with the IRAF task PHOT . After a curve of growth analysis on several sources we determined an optimum aperture size of 8 pixels with a suitable background annulus of 15 to 20 pixels. In order to check the photometry and to determine suitable selection criteria, we examined the 34 sources in common between the V band Keck image and our final V band HST globular cluster list. Similarly, 14 candidates were found in common between our final HST list and the Keck I band image. Although there was large scatter between the HST and Keck photometry at faint magnitudes, there was no obvious systematic bias. Our selection criteria are determined from the sample of 34 V band sources in common between the HST and the Keck frames. Due to HST's high spatial resolution, we are confident that the vast majority of sources that appear in the final HST list are bona fide GCs and hence use them to refine our Keck candidate list.

The following criteria were applied to the 615 objects in common between the Keck $B,\ V$ and I frames: (a) 21.5 < V < 25.0, (b) $2.5 < {\rm FWHM} < 12.0$ (c) ellipticity < 0.7. These selection cuts are shown in Fig. 2. As with our HST magnitude selection, the bright limit was chosen to include a population of young GCs while excluding bright foreground stars. Our faint magnitude cut-off was chosen in

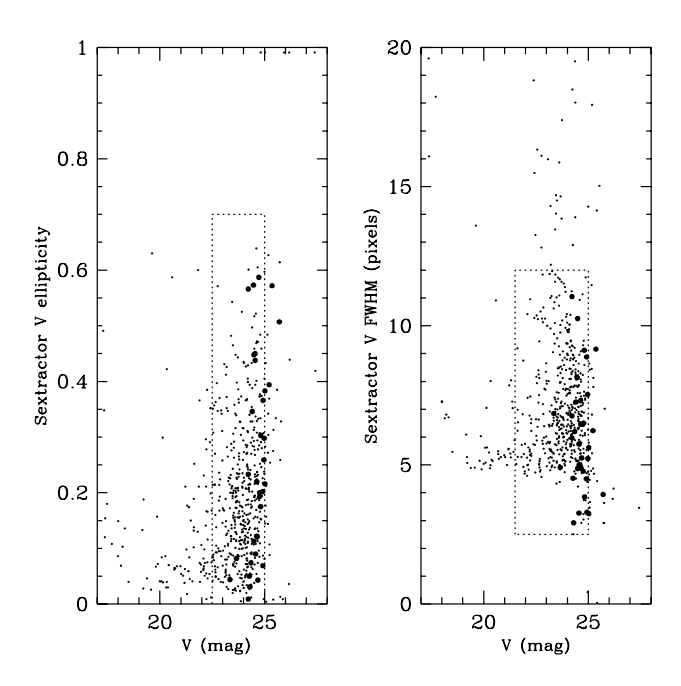


Figure 2. V band ellipticities and FWHMs of the initial sample of 615 globular cluster candidates in common between the Keck B, V and I band images. The selection cuts applied to this sample are represented by the dotted boxes (see text for details). The large solid circles are the 34 globular clusters in common with the final HST globular cluster list.

order to avoid introducing any colour bias into our results. After magnitude selection, 507 candidate GCs remained in our sample.

The selection using the SEXTRACTOR FWHM and ellipticity measures excluded a further 30 sources. These selection cuts were based on the shape parameters observed for the GCs in common with the HST list. We also excluded a further 25 sources because their x or y centre positions as determined by Phot deviated from those originally found by SEXTRACTOR by more than 2 pixels, and were thus liable to be misidentifications.

The full range of expected GC metallicities is -2.5 < [Fe/H] < +1.0. Using the Galactic colour–metallicity relation of Couture, Harris & Allwright (1990), this corresponds to a range in colour of 1.2 < B - I < 2.5. The errors in our photometry lead to an average error in colour of $\sim \pm 0.4$ mag. We thus decided to relax our final colour selection to 0.8 < B - I < 3.0. Our final colour selection is shown by the dotted box in Fig. 3. Here the range in V - I is defined as linear functions of B - I. This colour selection reduced our sample size down to a list of 352 objects. As a final stage in selection we performed a visual check of all the 352 candidate GCs in our colour selected list. From this inspection we rejected a further 40 sources that resembled galaxies (i.e. appeared diffuse and/or ellipsoidal) leaving a final list of 312 GCs.

Although these selection cuts are designed to reduce contamination to a minimum, there is always the concern that our final GC sample will still be contaminated by background galaxies and foreground stars. An estimate of the number of contaminating sources can be made by taking an image of a nearby 'blank' field. However, as we did not

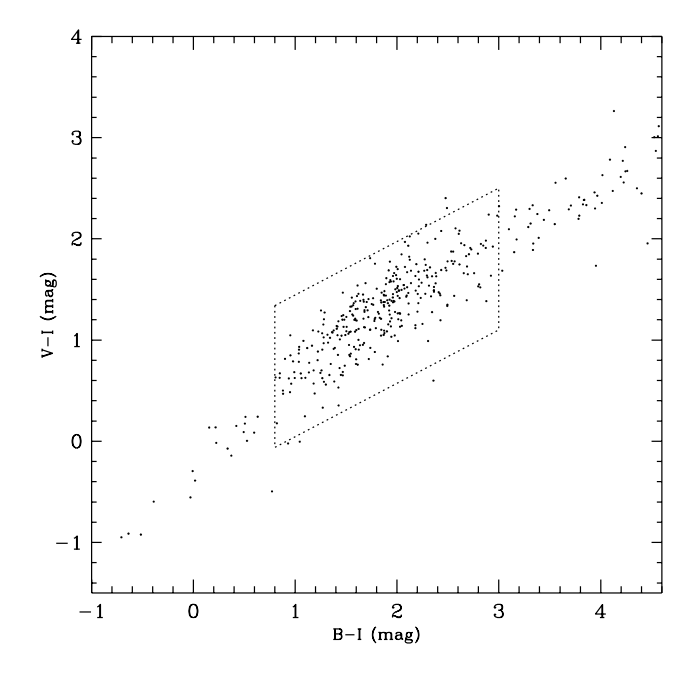


Figure 3. Colour–colour diagram for 452 globular clusters selected from our Keck data based on V magnitude, FWHM, ellipticity and $x,\ y$ position selection (see text). The dotted box represents the selection based on colour and contains 352 globular clusters.

have such an image, we had to use an alternative method. Bahcall & Soneira (1981) give the predicted stellar densities in 17 fields based on their model of the Milky Way. Using the star densities in the field closest in direction to our observations of NGC 1700 (field 13), and correcting for our field—of—view, we predict only 41 stars for our magnitude range of 21.5 < V < 25.0. Similarly we predict a total of 54 stars in our I band field (using limiting magnitudes of 20.5 < I < 23.5). The equivalent stellar density for the B band predicts only 29 stars in our field (assuming B band limiting magnitudes of 22.0 < B < 25.5). As our selection criteria requires sources to be in each of our B, V and I images, we conclude that \leq 29 foreground stars that could be present do not make up a significant contribution to our candidate sample.

Differential galaxy counts in the B band are given in fig. 1 of Koo & Kron (1992). From this we estimate a total of 1343 background galaxies in our B band frame down to our limiting magnitude of B = 25.5. Using Yoshii (1993) we estimate a total of 1130 galaxies in our I band frame (to I=23.5). Once again, as we selected only those sources in common between the B, V and I frames we can take the lower of these estimates as an indication of the number of contaminating galaxies in our list. These numbers are high compared to the 615 objects detected in common between our B, V and I frames, though the number of background galaxies actually detected will be significantly lower due to the incompleteness of the sample at faint magnitudes. Although potentially large in number, we show in Section 4.2.2 that the additional constraint of colour effectively excludes the majority of galaxies from our candidate GC list.

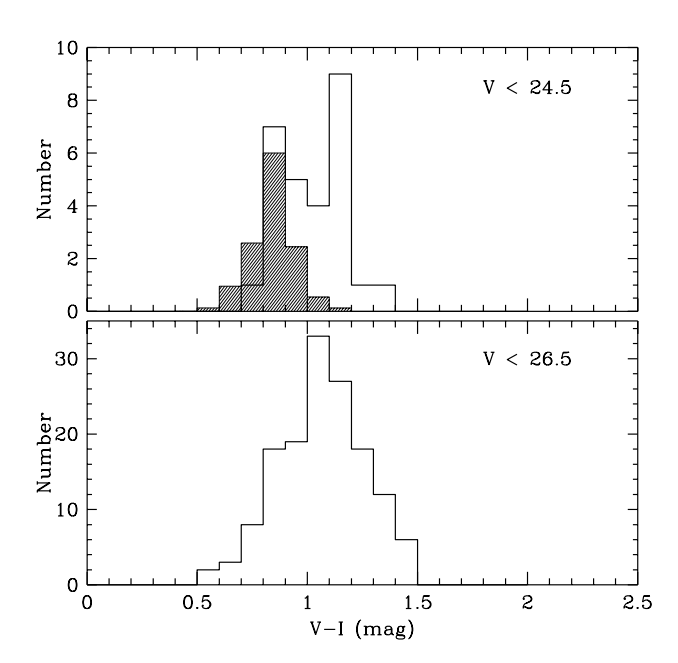


Figure 4. Histograms of NGC 1700 globular cluster V-I colours from HST images. The lower panel shows the V-I distribution of our whole sample. The peak is at V-I=1.07. The upper panel shows the colour distribution for those globular clusters with V<24.5 (which have colour errors of $\sim\pm0.1$ mag) and shows evidence for two populations, one at $V-I=0.85\pm0.05$ and one at $V-I=1.15\pm0.05$. The scaled $(V-I)_0$ colour distribution for Galactic GCs is shown as a shaded region and is consistent with the blue peak in our bright sub-sample.

4 RESULTS AND DISCUSSION

4.1 HST data

Two V-I histograms for the GCs in our HST sample are shown in Fig. 4. The lower panel shows the colour histogram for the whole 146 GC sample. There is a single peak at around V - I = 1.07, which is consistent with that of Whitmore et al. (1997), i.e. V - I = 1.05. The upper panel shows the V-I colour distribution for GCs in our sample that are brighter than V = 24.5. At V = 24.5, our typical error in colour is ~ 0.1 mag. Any fainter than this and the two distributions merge into a single broad peak due to photometric errors. For the bright sample, there is a suggestion of the presence of two peaks separated by $\Delta(V-I) = 0.30 \pm 0.07$, with one peak at $V-I = 0.85 \pm 0.05$ and one at $V-I=1.15\pm0.05$. As we have a small number of GCs brighter than V = 24.5 we use the dip statistic (see Hartigan & Hartigan 1985; Gebhardt & Kissler-Patig 1999) in order to confirm this bimodality. For our bright sample of HST GCs, the dip statistic indicates a probability of > 90 per cent that the distribution is not unimodal. The two peaks appear to have been 'washed out' at fainter magnitudes due to the photometric errors. The shaded region in this figure represents the $(V-I)_0$ histogram of Galactic GCs. This distribution shows a sharp peak at $(V-I)_0 \sim 0.9$, i.e. slightly bluer than the peak of the full sample but consistent with the blue peak of the V < 24.5 population.

An *HST* study of the NGC 1700 GC system prior to that of Whitmore et al. (1997) was performed by Forbes et al. (1996). Although only 39 GCs were detected, there was

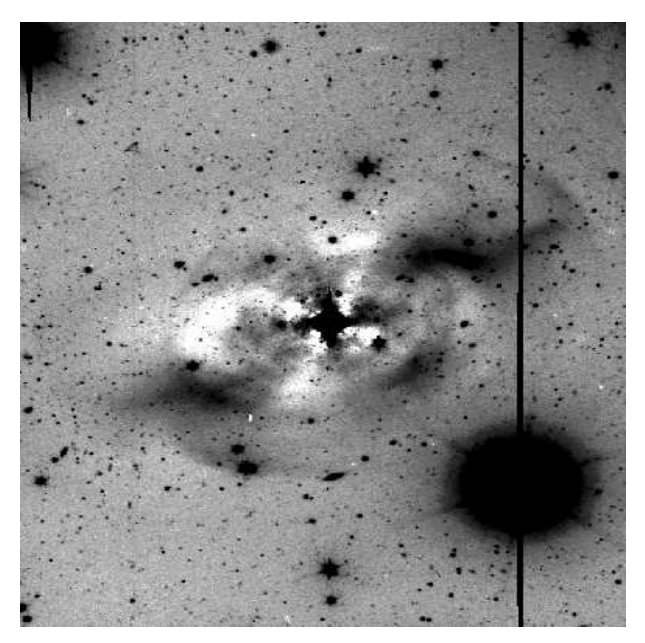


Figure 5. Residual map of NGC 1700 in the V band after subtraction of a galaxy model. Dark features represent excess light. The image reveals two roughly symmetric tail-like structures to the North-West and South-East of the galaxy. Note also the saturated region in the centre. The background has been raised to match the intensity at the outer modelling radius. The outermost modelled isophote is at a semi-major axis distance of 180 arcsec (45 kpc) from the centre.

a hint of possible bimodality in the V-I histogram with peaks at $V-I\sim0.9$ and $V-I\sim1.2$. Another HST observation of NGC 1700 was carried out by Richstone et al. (see Gebhardt & Kissler-Patig 1999). An analysis of these observations detected 27 GCs, again with two possible peaks in the colour distribution at $V-I\sim0.9$ and $V-I\sim1.2$. However, a statistical analysis of the V-I distribution detected no significant bimodality (Gebhardt & Kissler-Patig 1999). The positions of the peaks in Fig. 4 are consistent with those suggested by the previous observations mentioned above.

4.2 Keck data

4.2.1 Galaxy morphology and age estimates

In Fig. 5 we show the 'residual image' of NGC 1700 produced by subtracting the model from the 600 s V band image. Here the fine structure within the galaxy is better revealed. Most notable are the two broad, faint tidal tails or plumes visible to the North-West and South-East of the galaxy. In addition many GCs are apparent. The projected extent of the tidal features is about 165 arcsec (41 kpc) from the galaxy centre. A faint shell system is just visible in the central region (i.e. within the central ~ 25 arcsec) of the galaxy, as found in Forbes & Thomson (1992).

In Fig. 6 we show the profile of the 4th cosine (C4) parameter in the B, V and I bands for the long exposure images. The C4 term is generally positive at radii $\lesssim 30$ arcsec, representing discy isophotes. At greater than 30 arcsec the isophotes become strongly boxy, indicating an excess of light at $\sim 45^{\circ}$ from the major and minor axes. Fig. 5 shows that this is very probably due to some light from the tail-like

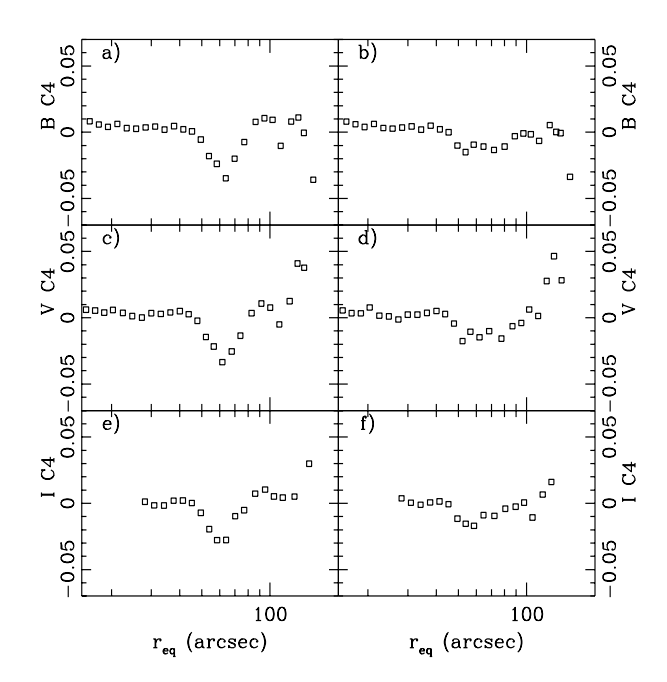


Figure 6. Radial profiles in the B, V and I bands of the 4th cosine term. a), c) and e) are profiles from the fits without masking the tails, while b), d) and f) are the profiles after masking. The boxiness at ~ 60 arcsec is significantly reduced by excluding the tidal tails from the galaxy model.

structures which remains in the galaxy model. To investigate this further, the 'tails' were masked out and the galaxy remodelled. Fig. 6 also shows the resulting C4 profiles after masking the tails. Note that the boxiness in the original fits has been greatly reduced in all cases (to less than 2 per cent deviation), indicating that the dominant cause of the boxiness at these radii is the tails. The tails themselves appear clearly brighter in the residual maps produced by subtraction of these models from the original images. This shows that without masking, some of the light from the tails is included in the model, modifying the fit parameters.

Keel & Wu (1995) constructed a 'merger sequence' from a sample of galaxies that are good candidates for ongoing mergers and remnants of mergers between two approximately equal mass disc galaxies. They assigned a 'merger stage' to each galaxy based upon dynamical crossing times, with zero age defined to be the point of nuclear coalescence. They noted that the fraction of galaxy starlight contained within the tails roughly anti-correlates with this merger stage. This allows us make a very rough estimate of the time-scale since the merger event that created the tails within NGC 1700.

This analysis was performed on the long exposure residual images. As we wanted to include as much of the tail light in the residual images as possible, we used the residual images produced by excluding the tails from the elliptical fit of the galaxy. As mentioned above, if the tails are not masked out during the fit, some of their light is included in the model, modifying the fit parameters and resulting in the subtraction of a significant amount of tail light from the galaxy image. The total flux contained within ~ 300 small circular apertures positioned on the tails was measured using the IRAF utility IMEXAMINE. This was used to derive a

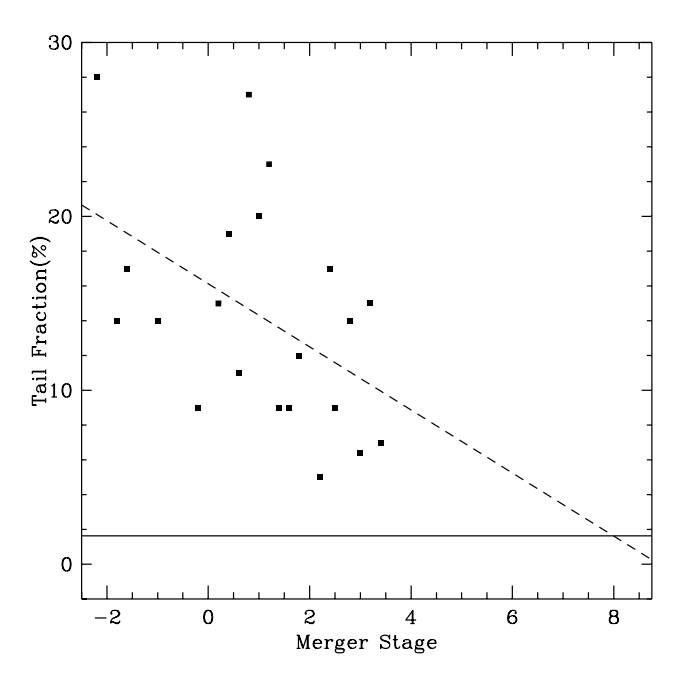


Figure 7. Tail fraction versus merger stage as derived from Keel & Wu (1995). The dashed line represents a linear least-square fitted to the sample of galaxies in the merger sequence of Keel & Wu (solid squares). The solid horizontal line represents the measured tail fraction of NGC 1700. From this method, we estimate that NGC 1700 is at a merger stage of 8.1 ± 3.8 , which roughly corresponds to an age of 3.2 ± 1.5 Gyr.

mean surface brightness for the tails, which was then multiplied by their total area (i.e. including the area missed due to contaminating bright sources). The resulting surface brightnesses were 26.6, 25.9 and 24.4 mag $\rm arcsec^{-2}$ for the $B,\,V$ and I bands respectively. The total light in the tails was divided by the total galaxy light to give the 'tail fraction'. We also roughly estimated the total tail light using polygon-shaped apertures. This method gave a similar result to the mean surface brightness method but included the light from contaminating point sources and was thus less reliable.

The tail fractions in the B, V and I bands were found to be 1.84, 1.64 and 1.72 per cent respectively. The tail fractions in Keel & Wu (1995) were derived in the V band, with a few exceptions. We thus use our V band tail fraction (which is similar to the B and I values) for NGC 1700 in the following analysis. We fitted a linear least-square to the points obtained from the Keel & Wu (1995) data. This fit is shown as a dashed line in Fig. 7. The solid horizontal line represents the measured V band tail fraction for NGC 1700. If we extrapolate the fit we find that the V band tail fraction measured for NGC 1700 corresponds to a merger stage of 8.1 ± 3.8 . The large error on this stage estimate is due to the scatter of the data points of Keel & Wu (1995). We also performed a quadratic fit on the Keel & Wu data. Extrapolating this fit yielded a stage comparable with the result using a linear least-square fit.

By comparing the spectroscopic (i.e. central starburst) ages of several galaxies in the Keel & Wu (1995) sample with their assigned merger stage, we determined the approximate time since nuclear coalescence. For the stage of NGC 1700,

the time since the central starburst and hence tail formation is approximately 3.2 ± 1.5 Gyr.

A lower limit for the age of the tidal tails can be estimated from the dynamical time-scale, i.e. $t_{\rm dyn} \sim (R/V)$. The projected distance of the tidal tails from the galaxy centre is about 165 arcsec (41 kpc), and the rotation velocity in the outer parts is ~ 50 km s⁻¹ (Bender et al. 1994). This gives a dynamical time of 0.8 Gyr, which is an underestimate if the tails do not lie in the plane of the sky; thus the tidal tails are > 0.8 Gyr old. This lower limit is consistent with the age derived from the fraction of galaxy light contained within the tails.

The presence of two symmetric tidal tails is generally taken to be a signature of a recent major merger involving two, approximately equal mass spiral galaxies (see e.g. Toomre & Toomre 1972). If the tidal features in Fig. 5 are indeed genuine tidal tails then we could conclude that NGC 1700 has experienced a major merger during its recent history. Alternatively, if the features are merely plumes of tidally disturbed material, the situation is less clear. While a major merger could not be ruled out, the situation of a disc galaxy merging into an existing elliptical would be possible.

4.2.2 Age estimates from globular cluster colours and magnitudes

We present in Fig. 8 the B-I colour histogram for NGC 1700 GCs from the Keck data. The histogram appears bimodal with a blue peak at $B-I=1.54\pm0.05$ and a second peak 0.44 ± 0.07 magnitudes redder at $B - I = 1.98 \pm 0.05$. This bimodality does not appear to be an artifact of the data binning and is still present if the histogram bin boundaries are changed. For the subsequent discussion and analysis we define the blue population as those GCs possessing $0.8 < B - I \le 1.75$ and the red population with colours 1.75 < B - I < 3.0. A statistical analysis using the KMM algorithm (Ashman, Bird & Zepf 1994) detects bimodality in the distribution with > 99 per cent confidence. The KMM algorithm assigned a colour cut between the blue and red populations of B - I = 1.8, thus confirming our initial visual estimate. The B-I distribution of GCs in the Milky Way is also shown in Fig. 8 (shaded area). The peak of this distribution is at $(B-I)_0 \sim 1.5$ which is similar to the peak of the blue population of NGC 1700.

Is the bimodality of the $B\!-\!I$ histogram evidence for two distinct GC populations in NGC 1700? In order to address this question, one has to consider the expected number of contaminating sources within our final sample. As the number of predicted stars before colour selection is small, we can immediately conclude that the contamination by foreground stars in our final sample is negligible. Another source of contamination is background galaxies. Our automatic and visual checks have removed obvious galaxies but it is possible that small, unresolved background galaxies remain. For our mean B magnitude of 24.5, we expect to be detecting sources out to a mean redshift of $z \sim 0.8$ (Koo & Kron 1992). At this redshift all morphological types of galaxies (with the exception of irregular types) have typical B-I colours in excess of 2.5. This is significantly redder than the peak of the red population and we can thus be fairly confident that the two peaks are real and due to two distinct populations of GCs. To support this view we performed photometry on

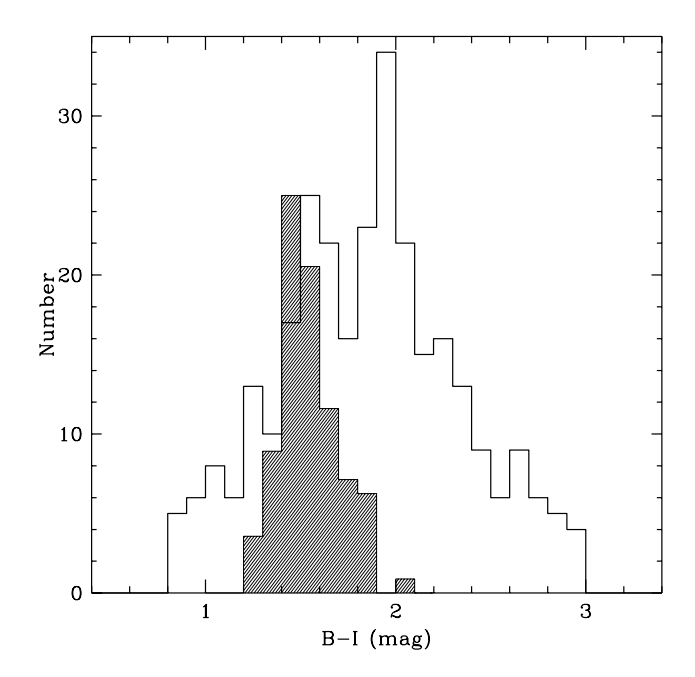


Figure 8. Histogram of B-I colours for our sample of 312 globular clusters in NGC 1700 from Keck images. Two peaks are apparent with centres at $B-I=1.54\pm0.05$ and $B-I=1.98\pm0.05$ respectively. The shaded area represents the $(B-I)_0$ histogram of globular clusters in the Milky Way.

13 galaxy-like objects that appeared in our initial list but were rejected during the selection process. The mean colour of these objects was $B-I=2.7\pm0.2$; significantly redder than the peak of our red population of objects in our final sample. Moreover, the mean FWHM value measured for these objects was 12.3 ± 1.2 pixels; greater than the upper cut-off used in our selection based on FWHM.

The study of globular cluster systems can reveal important information regarding the formation and evolution of the parent galaxy. The merger model of galaxy formation (Ashman & Zepf 1992; Zepf & Ashman 1993) makes a number of predictions about the properties of the GC system of the resultant galaxy. In this scenario, an elliptical galaxy is formed by the gas rich merger of two spiral galaxies. If our interpretation of two, roughly symmetric tidal tails in NGC 1700 is correct, then the galaxy has probably undergone such an event. If this is the case, the merger model predicts the formation of a new, metal rich population of GCs during the merger, which then reddens and fades with time. Post-merger ellipticals would thus be expected to possess a 'new' metal rich population and an old, metal poor population originating in the progenitor disc galaxies. Fig. 8 reveals evidence for two GC populations in NGC 1700. We next use the colours and magnitudes of these two populations to determine their age and metallicity properties.

The blue peak of our B-I histogram is roughly consistent with the peak of the B-I distribution of Galactic GCs (see Fig. 8). The Milky Way is likely to be a typical example of a progenitor in a present day gas-rich merger, thus indicating that we may assume that our blue peak in B-I is due to an old, metal poor population of GCs. Here we use the stellar population models of both Worthey (1994) and Bruzual & Charlot (2000) to predict the difference in magni-

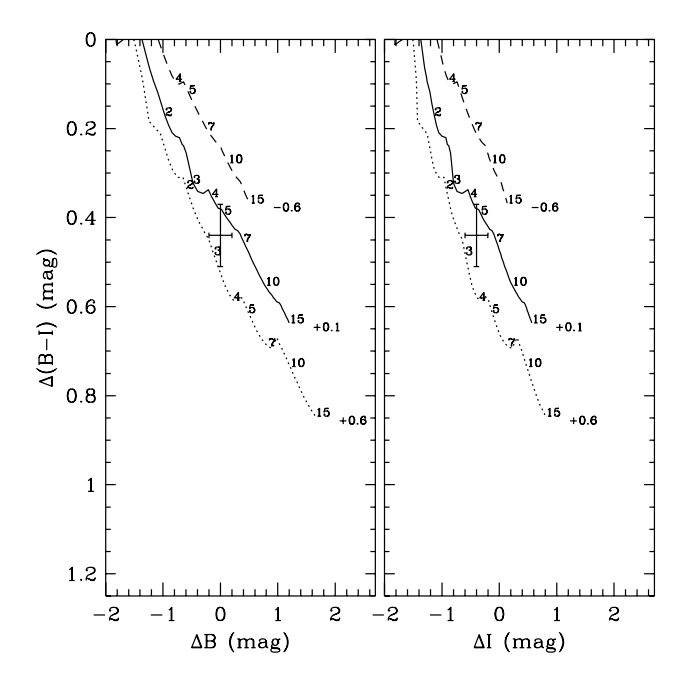


Figure 9. Evolution of $\Delta(B-I)$ vs. ΔB and ΔI with age from the models of Bruzual & Charlot (2000). The $\Delta(B-I)$ is defined as the colour difference between the red globular cluster population and a blue old, metal poor population with an age of 15 Gyr and [Fe/H] = -1.5. ΔB and ΔI are defined as the average magnitude difference between the two populations in the B and I bands respectively. The three tracks represent the evolution of the red population with metallicities as indicated on the end of each line. The cross shows the observed colour and magnitude difference between the two populations detected in NGC 1700, i.e. $\Delta(B-I) = 0.44 \pm 0.07$, $\Delta B = 0.0 \pm 0.2$ and $\Delta I = -0.4 \pm 0.2$. The predicted age of the red population is 2.5–5.0 Gyr with supersolar metallicity.

tude and colour for a population of young clusters, relative to an old, metal poor population with an age of 15 Gyr and [Fe/H] = -1.5. Fig. 9 shows the predicted differences in $\Delta(B-I)$ vs. ΔB and ΔI based on the models of Bruzual & Charlot (2000). Fig. 10 shows the equivalent colour and magnitude changes based on the models of Worthey (1994). In each case, three different metallicity tracks are shown. From Fig. 8, $\Delta(B-I) = 0.44 \pm 0.07$.

The ΔB and ΔI values correspond to the magnitude offset in the B and I bands between the young and old populations. These offsets were estimated from the cumulative B and I band GC luminosity functions for both the blue and red populations separately. These luminosity functions are shown in Fig. 11. To reduce the effect of photometric errors we considered only those GCs at least 0.5 mag brighter than the limiting magnitude in each band. The data has been normalised to the faint limit of our luminosity functions. The median magnitudes of the red and blue GCs considered were then calculated to allow us to determine the separation of the blue and red populations. The magnitude differences between the red and blue populations were determined to be $\Delta B = 0.0 \pm 0.2$ and $\Delta I = -0.4 \pm 0.2$ in the B and I bands respectively. The observed values with their associated errors are indicated by a cross on Fig. 9 and Fig. 10. Reference to the Bruzual & Charlot models shows that the red popu-

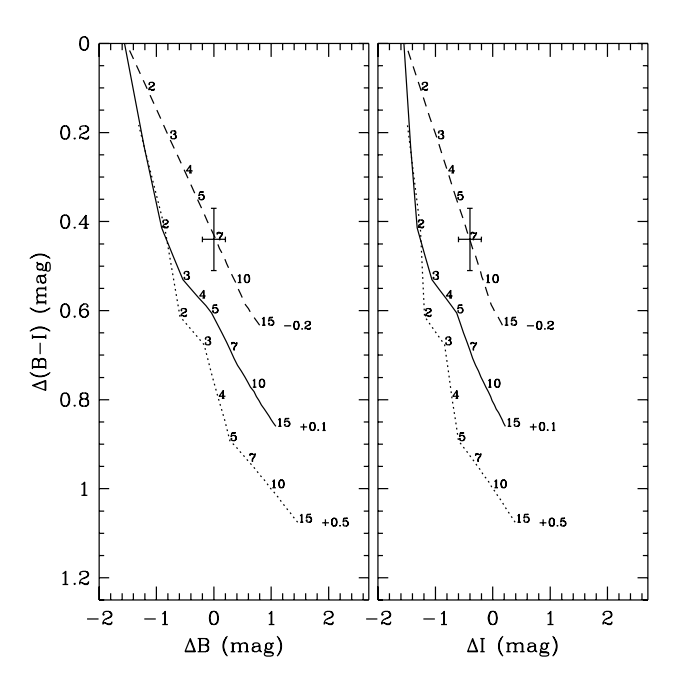


Figure 10. Evolution of $\Delta(B-I)$ vs. ΔB and ΔI with age from the models of Worthey (1994). The $\Delta(B-I)$ is defined as the colour difference between the red globular cluster population and a blue old, metal poor population with an age of 15 Gyr and [Fe/H] = -1.5. ΔB and ΔI are defined as the average magnitude difference between the two populations in the B and I bands respectively. The three tracks represent the evolution of the red population with metallicities as indicated on the end of each line. The cross shows the observed colour and magnitude difference between the two populations detected in NGC 1700, i.e. $\Delta(B-I) = 0.44 \pm 0.07$, $\Delta B = 0.0 \pm 0.2$ and $\Delta I = -0.4 \pm 0.2$. The predicted age of the red population is 5.0–8.0 Gyr with a subsolar metallicity.

lation is consistent with a young, metal rich population of globular clusters, i.e. with an age of 2.5-5.0 Gyr and supersolar metallicity ([Fe/H] $\sim +0.1$ to +0.6). A plot of ΔV vs. $\Delta(B-I)$, where $\Delta V = 0.1 \pm 0.2$ predicts a similar age and metallicity. It is interesting to note that the Worthey models predict significantly different values for the age and metallicity of the red GC population in the sense that they are older and more metal poor. From the Worthey models the age of the red GCs is 5.0–8.0 Gyr and $[Fe/H] \sim -0.2$. It thus appears that ages derived from GC colours and magnitudes are highly model dependent. However both models suggest that the red GCs are both younger and more metal rich than the blue population. We may suspect that [Fe/H]should be at least solar metallicity. In the merger model, the young population is thought to have formed from the relatively enriched gas in the spiral discs, in contrast to the old population which formed from metal poor gas. Moreover, the line strengths plotted in Fig. 13 (see Section 4.3 for details) imply for both models that the stellar metallicity of the last major starburst is $[Fe/H] \ge +0.5$. If the young GCs formed from the same gas, we would expect them to be metal rich as well, which in turn would favour the younger age of the Bruzual & Charlot models. However, if the young GCs were formed at an early stage of a merger-induced starburst then they could in principle be more metal poor than the present

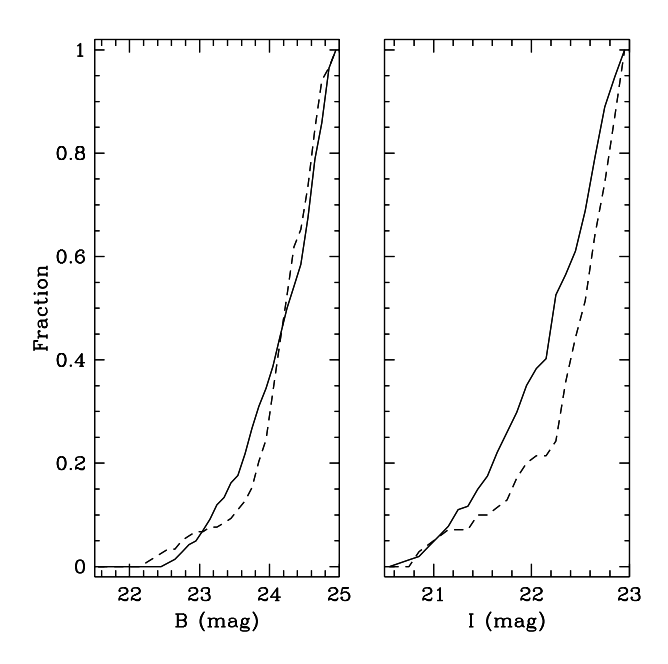


Figure 11. Normalised B and I band cumulative luminosity functions for the red (solid line) and blue (dashed line) populations of globular clusters. Only those globular clusters at least 0.5 magnitudes brighter than the corresponding limiting magnitudes are considered.

young stellar population (Fritze v. Alvensleben & Burkert 1995). To summarise, if we assume that the blue GCs are an old metal poor population, the red GCs are consistent with an age of 2.5–5.0 Gyr, assuming they have a metallicity of $0.0 \leq [Fe/H] \leq +0.5$. In the case that the red GCs are relatively metal poor, as suggested by the Worthey model tracks in Fig. 10 then a slightly older (5.0–8.0 Gyr) age is indicated. Infrared photometry or good spectra would help to resolve the age and metallicity independently.

From Section 4.1 we found evidence for bimodality in V-I with peaks at $V-I=0.85\pm0.05$ and $V-I=1.15\pm0.05$. A GC population with an age of 15 Gyr, [Fe/H]=-1.5 and V-I=0.85 will have $B-I\sim1.5$. This is consistent with the blue population seen in our B-I colour histogram. Similarly, a population with an age of 3 Gyr, [Fe/H]=+0.5 and V-I=1.15 is expected to have $B-I\sim1.9$, i.e. consistent with the red peak of our B-I distribution. It thus appears that the colours of the red and blue peaks in our B-I histogram are consistent with the the peaks hinted at in the $HST\ V-I$ colour distribution. The bimodality seen in independent data sets confirms the presence of two GC populations in NGC 1700.

We show in Fig. 12 the mean B-I colour of our GCs vs. galactocentric radius. The data are radially binned into 10 annuli, each of width 5.5 kpc (22 arcsec). The GC system of NGC 1700 does not show any significant correlation between colour and galactocentric distance. In particular the red (i.e. young) GCs are not preferentially concentrated towards the centre of the galaxy, as might have been expected from the merger origin for new GCs (Ashman & Zepf 1992; Zepf & Ashman 1993). A linear least-square fit to the radial colour bins gives a gradient consistent with zero. We do not detect any significant radial colour trend in the HST sample of GCs either, agreeing with the results of Whitmore et al.

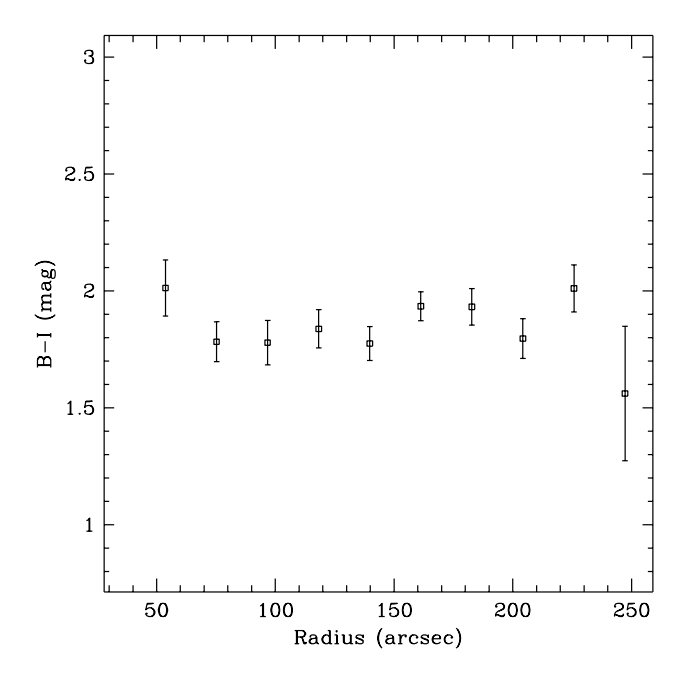


Figure 12. B-I colour vs. galactocentric radius for globular clusters in NGC 1700. The data are binned into annuli of width 22 arcsec. Error bars correspond to Poisson statistics. Note the lack of any strong trend in colour with radius.

(1997). This lack of an obvious radial trend is potentially a problem for the merger origin interpretation of the GCs, and deserves further consideration in any future studies. It is also interesting to note that the GC systems of several other ellipticals do show radial colour gradients in the sense that the red GCs are more centrally concentrated than the blue (see e.g. Geisler, Lee & Kim 1996; Forbes, Brodie & Grillmair 1997).

4.3 Other age estimates

Until recently, direct age dating of the stars in an elliptical was near-impossible due to the well known degeneracy of age-metallicity effects in old stellar populations. Spectral synthesis methods have now been developed (e.g. Worthey 1994; Bruzual & Charlot 2000) that show that combinations of certain spectral line indices can efficiently disentangle the effects of age and metallicity for young to intermediate age stellar populations. As well as stellar age dating, a number of other methods are available for NGC 1700. These estimates are shown for comparison in Table 1. We show a mean spectroscopic age based on the line strength data of Fisher, Franx & Illingworth (1996) and Gonzalez (1992), the age derived from the globular clusters by Whitmore et al. (1997), the 'fine structure age' of Schweizer & Seitzer (1992), the age from stellar dynamics (Statler, Smecker-Hane & Cecil 1996) and the age derived from the galaxy's deviation from the Fundamental Plane (see Forbes, Ponman & Brown 1998).

Table 1. Summary of age estimates for NGC 1700

Method	Age (Gyr)	Ref.
Globular clusters	4 ± 2 ?	Whitmore et al. (1997)
Fine structure	$< 6.0 \pm 2.3$	Schweizer & Seitzer (1992)
Stellar dynamics	2.7 - 5.3	Statler et al. (1996)
Tail fraction	3.2 ± 1.5	This work
Globular clusters	2.5 - 5.0	This work, Bruzual & Charlot models (2000)
Globular clusters	5.0 - 8.0	This work, Worthey (1994) models
Stellar spectroscopy	2.9 ± 0.3	This work, see text for details
Tail extent	> 0.8	This work
Fundamental Plane residual	1.2 ± 2.0	This work, Forbes et al. (1998b)
Best estimate	3.0 ± 1.0	This work

4.3.1 Ages from stellar population synthesis models

The spectroscopic age estimates in Table 1 are based on comparisons of observed absorption line strengths with singleburst stellar population models of Worthey (1994) and Bruzual & Charlot (2000). From these model grids, observed line strengths can be used to give estimates of the age and metallicity of the stellar component of a galaxy. We have used the $H\beta$ and [MqFe] line strengths from two sources, i.e. Fisher et al. (1996) and Gonzalez (1992). Fig. 13 shows the $[MgFe] - H\beta$ model grids with the observed values for NGC 1700 shown. In both panels, the solid circle indicates the observed line strengths from Fisher et al. (1996), whereas the open circle shows the line strengths from Gonzalez (1992). The apertures used in each case are $r_{\rm e}/10$ and $r_{\rm e}/8$ respectively because we are primarily concerned with the age of the central starburst. Using the Worthey models, the age derived from the Fisher et al. data is 2.7 ± 0.4 Gyr and the age from the Gonzalez data is 2.3 ± 0.3 Gyr. In both cases, the metallicity, [Fe/H] is $\geq +0.5$. Similar results are obtained by using the Bruzual & Charlot models. In this case the Fisher et al. data gives an estimated age of 3.5 ± 0.5 Gyr and the data of Gonzalez suggests an age of 2.9 ± 0.3 . Combining these results gives an average of 2.9 ± 0.3 Gyrs. Again both sets of data suggest a metallicity of $[Fe/H] \ge +0.5$. Note that this method measures a 'luminosity weighted mean age' of the central stellar population and is thus likely to be dominated by the young stellar population associated with the last episode of star formation. This may in turn be the result of a merger induced starburst.

4.3.2 Ages from globular clusters

Whitmore et al. (1997) employed a method similar to that used in Section 4.2.2 to derive GC ages. This method relies on the observed colour difference between two detected populations of GCs. Whitmore et al. (1997) detected only one population (at V-I=1.05). Their age of '4 ± 2 Gyr?' was derived from the non-detection of two distinct populations, though it is consistent with the other age estimates discussed herein. The non-detection appears to have arisen due to the small colour separation of the GC populations. Using the same data but restricting the sample to bright GCs, we have detected two separate populations as shown in Fig. 4. By including the whole sample (i.e. down to V=26.5) the two peaks merge into a single distribution.

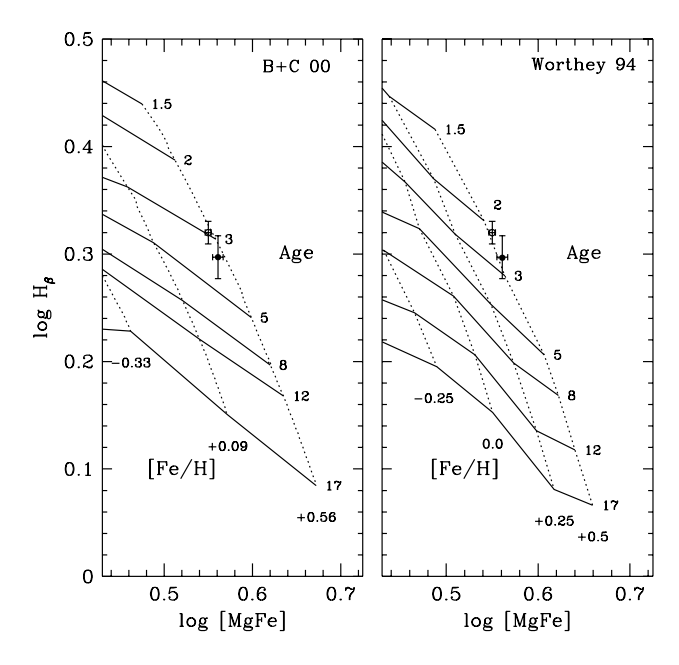


Figure 13. Worthey (1994) and Bruzual & Charlot (2000) model grids for $\log H\beta$ vs. $\log[MgFe]$. The solid lines are contours of constant age (in Gyrs) whereas the dashed lines represent lines of constant metallicity. The solid and open circles indicate the positions of NGC 1700 based on the line strength measurements of Fisher et al. (1996) and Gonzalez (1992) respectively.

4.3.3 Fine structure ages

Another method of estimating galaxy age was developed by Schweizer & Seitzer (1992). They defined a fine structure parameter, Σ , based on the amount of optical 'fine structure' present in a galaxy. This included a measure of the maximum boxiness of the galaxy isophotes, the number and strength of shells and tails and the presence or absence of 'X-structure'. The values of Σ for the galaxies in their sample ranged from 0 for galaxies with no fine structure to 7.6 indicating the largest amount of fine structure observed. NGC 1700 was assigned a value of 3.70. They found that Σ correlated with a galaxy's residual from the mean colour-magnitude relation. Using this fact and relating galaxy colours to ages via a star formation model, they estimated the time since the merger event. We quote their most representative age of 6.0 Gyr with an error of ± 2.3 Gyr in Table 1. We note however, that the models used in Schweizer & Seitzer (1992) assumed a solar metallicity starburst. If the stellar population is supersolar, as suggested by Fig. 13, then the Schweizer & Seitzer (1992) age is expected to be a slight over-estimate.

4.3.4 Dynamical considerations

The age estimate of Statler et al. (1996) comes from measurements of the stellar velocity field of NGC 1700. They found that within $\sim 2.5r_{\rm e}$ (8.8 kpc) the galaxy is kinematically well mixed. This constrains the time since the last major merger event to be ≥ 2.7 Gyr to allow sufficient time for phase mixing and differential precession. Their observations also define an upper limit for the time since the merger. The asymmetric photometric and kinematic signatures at larger radii preclude a merger age greater than 5.3 Gyr, otherwise these features would have relaxed and disappeared. Thus we quote an age of 2.7–5.3 Gyr. The same paper argues that the counter rotating core and boxy features (the latter of which we attribute to the tidal tail-like structures) could not have been created by the same merger event and that the observed form of NGC 1700 must have arisen from the merger of at least three separate stellar systems. However, it was not clear whether these events occurred sequentially or simultaneously. If the two tail-like structures are indeed genuine tidal tails this would suggest that the history of NGC 1700 has included at least one major merger event involving two approximately equal mass disc galaxies. If the kinematically distinct core (KDC) was formed prior to this event it would have probably been disrupted during the ensuing violent relaxation processes. If the KDC was indeed formed by a separate process it must have resulted from a subsequent minor merger (e.g. Balcells & Quinn 1990) or an interaction (see Thomson & Wright 1990) some time after the major merger event that created NGC 1700 and its tails. Neither of these suggestions are very appealing. Alternatively, the tidal structures seen in Fig. 5 could be interpreted as plumes which have arisen from the infall of a small disc galaxy into a pre-existing elliptical.

4.3.5 Scatter from the Fundamental Plane

A recent study by Forbes et al. (1998b) showed that a galaxy's deviation from the Fundamental Plane (FP) correlated with its age, albeit with large scatter. The FP residual is defined as $R(\sigma_0, M_{\rm B}, \mu_{\rm e}) = 2\log(\sigma_0) + 0.286M_{\rm B} + 0.2\mu_{\rm e} - 3.101$ (Prugniel & Simien 1996). Young ellipticals fall below the FP (i.e. have negative residuals) and evolve towards it until they lie on the FP at an age of about 10 Gyr. Older ellipticals tend to lie above the FP. It is thus possible to use the FP residual to approximately age date an elliptical galaxy. The FP residual for NGC 1700 is $R(\sigma_0, M_{\rm B}, \mu_{\rm e}) = -0.37$. This corresponds to an age of 1.2 ± 2.0 Gyr based on the fit in Forbes et al. (1998b). This is slightly younger but comparable to the other age estimates discussed in this section.

4.3.6 Comparison of various age estimates

Before directly comparing the different age estimates, one should bear in mind that the dating methods may be measuring different time-scales and may have large errors associated with them. As mentioned above, the stellar spec-

troscopy methods measure the central 'luminosity weighted average age' which means they are dominated by the last burst of star formation, although the old stellar population also contributes. Thus the true age of the starburst may be slightly less than the spectroscopic age. The young GCs were possibly formed in the same star formation event as the galaxy starburst, and as such should give a similar age as the stellar spectroscopy. The age estimate from the Forbes et al. (1998b) trend is also based on a star formation time-scale.

The stellar dynamics, fine structure and tail fraction ages estimate the time since the last merger event. The 'dynamical/structural' estimates are reasonably consistent with the 'starburst' ages, indicating a relatively young age for NGC 1700, and suggesting that the merger was a gaseous one. Mihos & Hernquist (1996) have shown that in a merger between two spirals with bulges the main starburst occurs at the time of nuclear coalescence while the tails form ~ 0.5 Gyr earlier. If this is the case, we might expect the 'dynamical/structural' age estimates to be slightly higher than the 'starburst' ones. We have decided to adopt an age for NGC 1700 of 3.0 ± 1.0 Gyr as our best estimate. This may also correspond to the time since the nuclei of the progenitors merged.

4.4 Globular cluster spatial properties and specific frequency

4.4.1 Spatial distribution

Given the field-of-view, our Keck observations are ideal for defining the outer reaches of the GC system. We have calculated the surface density (SD) profile for the GC system in the Keck images within 9 annuli centred on the galaxy. For objects in the corner of the CCD, the SD was calculated by taking into account the area of the annulus 'missing' off the edges of the chip. This method allowed us to calculate the density out to a radius of 232 arcsec (~ 60 kpc). The resulting surface density profile is shown in Fig. 14. The error bars simply reflect the Poisson errors on the number of GCs in each bin. At large radii the surface density decreases like a power-law with radius (open squares). At radii < 140 arcsec however, there appears to be a significant deficit in the number of GCs detected in our Keck images (shown by open circles). The most likely cause for this is the fact that GCs at small radii are superimposed on the bright body of the galaxy which also possesses a steep radial gradient at these distances. Although an elliptical model of the galaxy was subtracted from each of the initial images, this effect seems to have caused a reduction in our ability to detect GCs as our HST surface density continues to rise towards the centre at these radii as shown in Fig. 15. In addition, we were unable to detect GCs in the Keck images within the central 33 arcsec due to the large saturated region at the centre of the I band image. To quantify the outer SD profile of the GCs detected in our Keck images, we fitted the outermost points in Fig. 14 with a function of the form $\rho = \rho_0 r^{\alpha}$. This fit is shown by the dashed line in Fig. 14. We find that $\rho_0 = 0.5 \pm 3.3$ and $\alpha = -1.07 \pm 0.25$. Background contamination of the sample would add a constant SD level to the profile. Although this contamination is likely to be small, ideally it would be taken into consideration when computing the fit. However, our data are not sufficient to calculate the

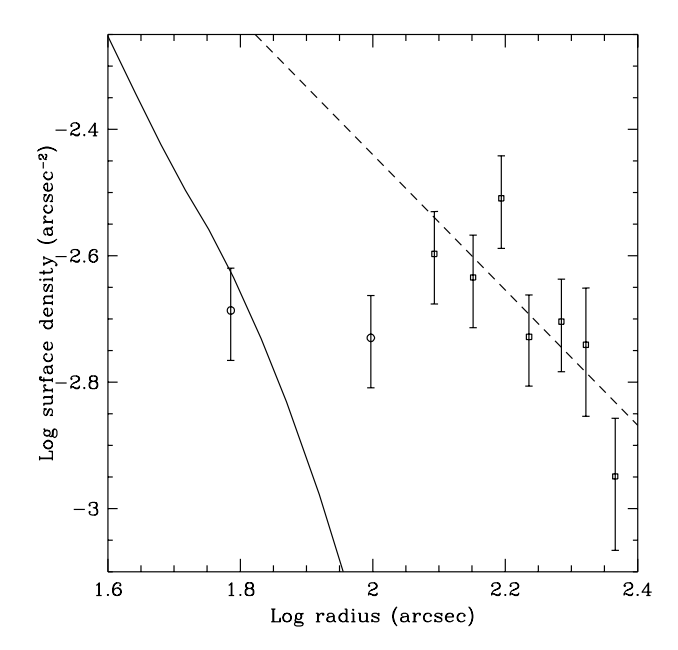


Figure 14. Surface density profile of our final Keck sample of globular clusters in NGC 1700. The significant deficit of Keck globular clusters within a radius of ~ 140 arcsec (open circles) is likely to be an artefact of our galaxy modelling process. At larger radii, the surface density profile resembles a power-law (open boxes). A power-law fitted to these outer points is shown as the dashed line. The solid line is the stellar intensity profile of the underlying galaxy and has a significantly steeper slope than the globular cluster surface density distribution.

level of contamination and the calculated slope of the profile should be treated with caution. The solid line in Fig. 14 represents the stellar profile of the galaxy. The galaxy profile used is not in the usual units of surface brightness but has been converted to $\log(intensity)$ and arbitrarily shifted in the Y direction to allow simple comparison of the slopes. We measure a slope of -1.9 ± 0.1 for the galaxy profile using the measured intensities at all radii. It thus appears that the GC profile is flatter than the underlying stellar profile.

In order to investigate the SD profile within the central regions of the galaxy, we use the HST images. This profile is shown in Fig. 15 after correction for the areas of the annular bins missing from the WFPC2 field-of-view. Each annulus contains ~ 25 GCs with the exception of the two inner bins which contain ~ 10 GCs. We find that the HST surface density follows a power-law profile exterior to $r \sim 11$ arcsec (i.e. the outer 6 data points). We again fitted these points with a function of the form $\rho = \rho_0 r^{\alpha}$ and find $\alpha = -0.90 \pm 0.15$ and $\rho_0 = 0.27 \pm 0.19$ GC arcsec⁻². The slope of this fit is within the range of values measured for other ellipticals by other authors (e.g. Forbes et al. 1997) and also consistent with the slope calculated from the Keck sample. Also shown in Fig. 15 is the stellar profile of the galaxy. This has a slope of -1.9 ± 0.1 . The GC profile is significantly flatter than that of the galaxy, which is often the case in other systems (e.g. Grillmair, Pritchet & van den Bergh 1986; Harris 1986; Lauer & Kormendy 1986; Forbes et al. 1998a; Ashman & Zepf 1998). Within ~ 11 arcsec there is evidence for a flattening of the profile indicating the presence of a 'core region'. The core radius of the NGC 1700

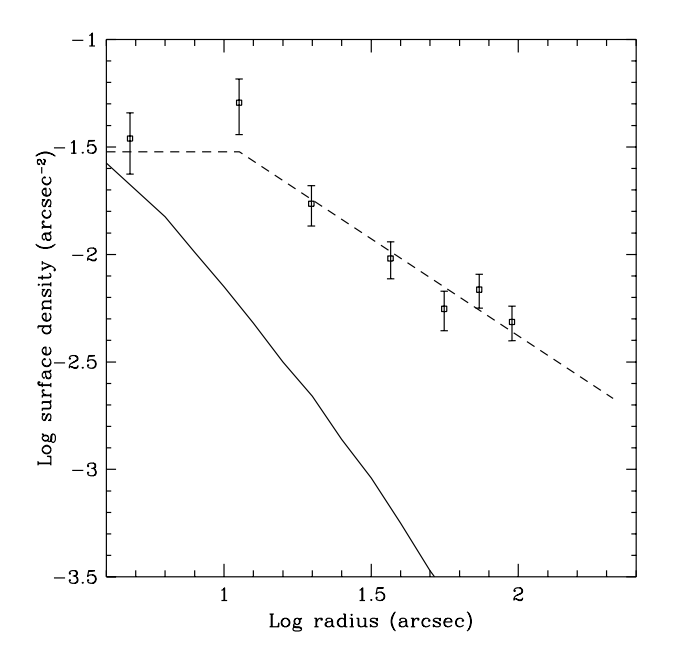


Figure 15. Surface density profile of our final *HST* sample of globular clusters in NGC 1700 (open squares). The dashed line is a power-law fitted to the data with a flat core region inside a radius of 11 arcsec. The solid line is the stellar intensity profile of the underlying galaxy and has a significantly steeper slope than the globular cluster surface density distribution.

GC distribution was also measured by Forbes et al. (1996) to be 2.7 ± 1.6 kpc corresponding to ~11 arcsec, although only 39 GCs were detected. The presence of a core region is also commonly seen in other ellipticals and Forbes et al. (1996) define a relationship between GC system core radius and parent galaxy luminosity. This relation is in the sense that more luminous ellipticals have more extended GC systems. An elliptical with the luminosity of NGC 1700 (i.e. $M_{\rm V}=-22.47$) is expected to have a core radius of ~3 kpc, corresponding to ~12 arcsec, although there is a large uncertainty on this value (Forbes et al. 1996). Our data are thus consistent with the expectation from other ellipticals and with the previous direct measurement of the NGC 1700 GC system core radius.

4.4.2 Total number of globular clusters

We next make an estimate of the total number, $N_{\rm T}$, of GCs possessed by NGC 1700. In order to estimate $N_{\rm T}$ we integrate under the surface density profile out to some limiting radius. We will assume a flat profile interior to our second data point ($r=11.3~{\rm arcsec}$) with log(SD) = -1.52 (as shown in Fig. 15), although this assumption has little effect on the final calculation. Outside this radius we assume a power-law profile. The faint magnitude limit for our Keck data ($V\sim25$) is much brighter than the expected peak magnitude of a standard GC luminosity function at the distance of NGC 1700. Thus the correction for incompleteness would be very large. In addition, the Keck data has a higher contamination rate than HST which is difficult to account for without a corresponding 'blank sky' image. We therefore integrate under the power-law fitted to the HST

points only, for which we are confident there is very little contamination, and we expect a much smaller incompleteness correction. We use the Keck data to help us to define a reasonable outer limiting radius.

The dominant sources of error in determining $N_{\rm T}$ are the choice of the outer limiting radius and the correction for incompleteness at faint magnitudes. Fig. 14 indicates that the surface density declines out to a radius of ~ 210 arcsec outside of which there is a large drop in surface density. This suggests that the limit of the GC distribution has been reached. We thus chose to integrate out to 210 arcsec, which corresponds to a galactocentric distance of 50 kpc, in order to calculate the total number of GCs within this radius. This limiting radius is comparable to the extents of the GC systems seen in other ellipticals (see e.g Hanes & Harris 1986). The resulting number of GCs was then corrected to account for the lack of completeness in the HST sample at faint magnitudes. Based on our limiting magnitude we estimate this correction factor to lie in the range of 2-3, thus adopting a correction factor of 2.5, with an uncertainty of ± 0.5 . We estimate that we are detecting roughly (40 ± 8) per cent of the total GC system within the limits of the HST field-of-view. We multiplied the number of GCs calculated from the SD profile by 2.5 to obtain a completeness corrected value for $N_{\rm T}$ within 50 kpc of $N_{\rm T}=1320\pm270$. Our value is greater than that found by Whitmore et al. (1997) who estimated a total number of 528 ± 48 GCs. However they considered only those GCs out to the radius of the HST field-of-view, whereas our Keck data indicates that the GCs are still present out to ~ 200 arcsec.

4.4.3 Specific frequency

The globular cluster specific frequency, S_N , is a useful quantity as it can provide valuable constraints on the formation mechanisms of the GC system as well as providing information on the formation history of the parent galaxy and potentially the nature of the progenitor spirals. From N_T , we calculate the total GC specific frequency $S_N(\text{total})$ within 50 kpc from the galaxy centre, from the following relation (Harris & van den Bergh 1981)

$$S_N(\text{total}) = N_T \times 10^{0.4(M_V + 15)}$$

where $M_{\rm V}$ is the absolute magnitude of the stars associated with the population of GCs in question. In the case of $S_N({\rm total})$, the required luminosity is the absolute magnitude of the galaxy, i.e. $M_{\rm V}=-22.47$. We will assume a 20 per cent error in the distance to NGC 1700, corresponding to an error in $M_{\rm V}$ of 0.4 mag. This yields for $N_{\rm T}=1320\pm270$, a total specific frequency of $S_N({\rm total})=1.4^{+1.0}_{-0.6}$. Elliptical galaxies have a wide range of GC specific frequencies. The mean value for ellipticals in the compilation of Ashman & Zepf (1998) is $S_N=5.1\pm0.6$, though there are a couple of cases of ellipticals with S_N values less than 1.0. Although possessing large errors, our $S_N({\rm total})$ is relatively low compared to most typical ellipticals and is more consistent with disc galaxies.

It is clear from the age estimates discussed herein that NGC 1700 is a relatively young galaxy. Will the GC population eventually come to resemble those seen around typical old ellipticals? To address this question we use the Worthey

models to predict the total specific frequency once sufficient time has passed for NGC 1700 to have an age comparable to those of typical elliptical galaxies today. Old, present day ellipticals have stellar population ages of 10-15 Gyr so in order to make this comparison we compute the luminosity of a young starburst component after it has aged by 10 Gyr. As the mass of the starburst is uncertain, we consider two cases: Firstly we assume a starburst that represents 10 per cent of the galaxy by mass and is embedded in a 10 Gyr population making up the remaining 90 per cent of the galactic stellar mass. After 10 Gyr, the models indicate that the young stellar population will fade by $\Delta V = 1.48$ mag (for an [Fe/H] = +0.5 population). As this population constitutes only 10 per cent of the galaxy mass however, the global fading is only $\Delta V = 0.18$ mag. This results in a predicted $S_N(\text{total})$ of ~ 1.6 , which is still lower than that expected for most typical present day ellipticals and suggests that NGC 1700 may form a relatively 'globular cluster poor' elliptical galaxy. If the starburst fraction is less than 10 per cent (as might be expected in an elliptical plus spiral merger), then the global fading is further reduced.

Secondly, we consider a starburst that constitutes 50 per cent of the galaxy mass. The remaining 50 per cent is made up of the old stellar population. After 10 Gyr, the fading of the young stellar population results in a global fading of $\Delta V = 0.81$ mag. The $S_N(\text{total})$ predicted after 10 Gyr is ~ 2.8 . This is more consistent with elliptical galaxy specific frequencies, though still lower than the mean S_N value calculated from Ashman & Zepf (1998).

The merger model of GC formation by Ashman & Zepf (1992) states that the number of new globular clusters formed in a merger will be proportional to the available gas mass, and that most 'normal' old ellipticals were formed from progenitors which were relatively gas—rich compared to present day spirals. It is interesting to note therefore that if one accepts the merger hypothesis and the fact that NGC 1700 is a relatively young elliptical, its GC specific frequency may be expected to be relatively low. Note, however that our 'predicted' values of S_N should be considered as very approximate as there is not only an inherent difficulty in estimating our sample completeness (and hence the number of GCs), but also a large uncertainty associated with the assumptions made regarding the future evolution of the galaxy luminosity.

5 CONCLUSIONS

We have presented results from new B, V and I band imaging of NGC 1700, taken using the Keck telescope and reanalysed previous HST imaging. From the morphology of the galaxy and photometry of its globular cluster system, we have derived new estimates of the galaxy age.

Subtraction of an elliptical model from the Keck images revealed the presence of two symmetric tidal tail-like structures extending ~ 40 kpc to the North-West and South-East of the galaxy. The presence of tidal tails is thought to be a classic signature that a galaxy has undergone a merger event, involving the collision of two spiral galaxies during the last few Gyr. If the observed tidal features are indeed genuine tidal tails, then this would suggest that NGC 1700 has undergone a major merger event during its recent his-

tory. If they are merely plumes or other fine structure, then the situation of a disc galaxy merging with an elliptical is also possible. Based on the fraction of galaxy light contained within these tails we have estimated their age at 3.2 ± 1.5 Gyr. We have also shown that NGC 1700 possesses boxy isophotes for radii of 7.5 < r < 20.0 kpc, and that this boxiness is largely caused by the presence of the tail structures.

From the HST imaging, we detected 146 globular clusters. Of these, 34 were in common with our GC candidates detected in the Keck data. We then used these common GCs to refine our Keck GC selection. After further restricting our sample in magnitude and colour we obtained a final Keck object list of 312 GCs. These show a bimodal colour distribution with peaks at B-I=1.54 and 1.98. The colour of the blue population is consistent with that of Galactic GCs. Assuming that the blue population is indeed an old metal poor system and measuring the offset in magnitude and colour between the two populations, we find that the red GCs are younger and more metal rich. The Bruzual & Charlot (2000) stellar population models suggest that the red population is 2.5-5.0 Gyr old and has super-solar metallicity. The equivalent models of Worthey (1994) predict a significantly older age (5.0–8.0 Gyr) and a lower metallicity ($[Fe/H] \sim -0.2$). The bimodality in B-I is supported by a hint of bimodality seen in the V-I colours from HST data.

We discuss other age estimates from the literature based on fine structure, globular cluster colours, Fundamental Plane residuals, stellar dynamics, and spectroscopic line strengths. We find that, although possessing significant errors, the various age estimates generally indicate a young age for NGC 1700 of about 3.0 ± 1.0 Gyr. The fact that the 'dynamical/structural' and 'star formation' ages are similar suggests that NGC 1700 has undergone an episode of enhanced star formation triggered by a merger event, which may have created the galaxy itself.

The surface density profile of GCs reveals a flatter (i.e. more extended) profile than the underlying galaxy starlight. The total number of GCs and present total specific frequency are estimated to be $N_{\rm T}=1320\pm270$ and $S_N(\text{total}) = 1.4^{+1.0}_{-0.6}$ respectively. The value for $S_N(\text{total})$, even considering the large errors, is quite low compared to the majority of typical ellipticals and is more consistent with spiral galaxies. We predict that after 10 Gyr the total S_N will have increased to a maximum of ~ 2.8 if NGC 1700 has undergone a starburst that constitutes 50 per cent of its stellar mass. This is consistent with low S_N ellipticals. If the starburst constitutes only 10 per cent of the total stellar mass, the predicted S_N is somewhat lower at $S_N \sim 1.6$. This suggests that NGC 1700 will form a relatively 'globular cluster poor' elliptical galaxy once it reaches a comparable age to typical 'old' ellipticals.

ACKNOWLEDGMENTS

We thank Trevor Ponman, Alejandro Terlevich and Edward Lloyd—Davies for help and useful discussions. We also thank the referee, Keith Ashman for his helpful comments.

Some of the data presented herein were obtained at the W. M. Keck Observatory, which is operated as a scientific partnership among the California Institute of Technology, the University of California and the National Aeronautics

and Space Administration. The Observatory was made possible by the generous financial support of the W. M. Keck Foundation.

This work was also based on observations with the NASA/ESA *Hubble Space Telescope*, obtained from the data archive at the Space Telescope Science Institute, which is operated by the Association of Universities for Research in Astronomy, Inc. under NASA contract No. NAS5-26555.

Part of this research was funded by NATO Collaborative Research grant CRG 971552.

REFERENCES

Ashman K. M., Zepf S. E., 1992, ApJ, 384, 50

Ashman K. M., Zepf S. E., 1998, Globular Cluster Systems. Cambridge University Press, Cambridge

Ashman K. M., Bird C. M., Zepf S. E., 1994, AJ, 108, 2348

Bahcall J. N., Soneira R. M., 1981, ApJS, 47, 357

Balcells M., Quinn P. J., 1990, ApJ, 361, 381

Bender R., Burstein D., Faber S. M., 1992, ApJ, 399, 462

Bender R., Saglia R. P., Gerhard O. E., 1994, MNRAS, 269, 785

Bertin E., Arnouts S., 1996, A&AS, 117, 393

Bruzual G. A., Charlot S. 2000. In preparation

Couture J., Harris W. E., Allwright J. W. B., 1990, ApJS, 73, 671

de Vaucouleurs G., de Vaucouleurs A., Corwin Jr. H. G., Buta R. J., Paturel G., Fouque P., 1991, *Third Reference Catalogue of Bright Galaxies*. Springer, Berlin, (RC3)

Fisher D., Franx M., Illingworth G., 1996, ApJ, 459, 110

Forbes D. A., Thomson R. C., 1992, MNRAS, 254, 723

Forbes D. A., Franx M., Illingworth G. D., Carollo C. M., 1996, ApJ, 467, 126

Forbes D. A., Brodie J. P., Grillmair C. J., 1997, AJ, 113, 1652

Forbes D. A., Grillmair C. J., Williger G. M., Elson R. A. W., Brodie J. P., 1998a, MNRAS, 293, 325

Forbes D. A., Ponman T. J., Brown R. J. N., 1998b, ApJ, 508, L43

Franx M., Illingworth G., Heckman T., 1989a, ApJ, 344, 613

Franx M., Illingworth G., Heckman T., 1989b, AJ, 98, 538

Fritze v. Alvensleben U., Burkert A., 1995, A&A, 300, 58

Gebhardt K., Kissler-Patig M., 1999, AJ, 118, 1526

- Geisler D., Lee M. G., Kim E., 1996, AJ, 111, 1529
- Gonzalez J., 1992, PhD thesis, University of California
- Goudfrooij P., Hansen L., Jorgensen H. E., Norgaard-Nielson H. U., de Jong T., van den Hoek L. B., 1994, A&AS, 104, 179
- Grillmair C., Pritchet C., van den Bergh S., 1986, AJ, 91, 1328
- Hanes D. A., Harris W. E., 1986, ApJ, 309, 564
- Harris W. E., van den Bergh S., 1981, AJ, 86, 1627
- Harris W. E., 1986, AJ, 91, 822
- Hartigan J. A., Hartigan P. M., 1985, Ann. Stat., 13, 70
- Holtzman J. A., Burrows C. J., Casertano S., Hester J. J., Trauger J. T., Watson A. M., Worthey G., 1995, PASP, 107, 1065
- Keel W. C., Wu W., 1995, AJ, 110, 129
- Koo D. C., Kron R. G., 1992, ARA&A, 30, 613
- Landolt A. U., 1992, AJ, 104, 340
- Lauer T. R., Kormendy J., 1986, ApJ, 303, L1
- Mihos C. J., Hernquist L., 1996, ApJ, 464, 641
- Oke J. B. et al., 1995, PASP, 107, 375
- Poulain P., 1988, A&AS, 72, 215
- Prugniel P., Simien F., 1996, A&A, 309, 749
- Sandage A., Tammann G. A., 1981, A Revised Shapley-Ames Catalog of Bright Galaxies. Carnegie Institution, Washington, (RSA)
- Schweizer F., Seitzer P., 1992, AJ, 104, 1039
- Statler T. S., Smecker-Hane T., Cecil G. N., 1996, AJ, 111, $1512\,$
- Thomson R. C., Wright A. E., 1990, MNRAS, 247, 122
- Toomre A., Toomre J., 1972, ApJ, 178, 623
- Whitmore B. C., Miller B. W., Schweizer F., Fall S. M., 1997, AJ, 114, 1797
- Worthey G., 1994, ApJS, 95, 107
- Yoshii Y., 1993, ApJ, 403, 552
- Zepf S. E., Ashman K. M., 1993, MNRAS, 264, 611